Conformational Changes in Human Hepatitis C Virus NS3 Protease upon Binding of Product-Based Inhibitors†

Elisabetta Bianchi,*,‡ Stefania Orrù,§,|| Fabrizio Dal Piaz,§ Raffaele Ingenito,‡ Annarita Casbarra,§ Gabriella Biasiol,‡ Uwe Koch,‡ Piero Pucci,§ and Antonello Pessi‡

Istituto di Ricerche di Biologia Molecolare P. Angeletti (IRBM), Via Pontina Km 30.600, 00040 Rome, Italy, and Centro Internazionale di Servizi di Spettrometria di Massa, CNR-Università di Napoli Federico II, Via Pansini 5, 80131 Napoli, Italy

Received May 28, 1999

ABSTRACT: One of the most promising approaches to anti-hepatitis C virus drug discovery is the development of inhibitors of the virally encoded protease NS3. This chymotrypsin-like serine protease is essential for the maturation of the viral polyprotein, and processing requires complex formation between NS3 and its cofactor NS4A. Recently, we reported on the discovery of potent cleavage product-derived inhibitors [Ingallinella et al. (1998) *Biochemistry 37,* 8906−8914]. Here we study the interaction of these inhibitors with NS3 and the NS3/cofactor complex. Inhibitors bind NS3 according to an induced-fit mechanism. In the absence of cofactor different binding modes are apparent, while in the presence of cofactor all inhibitors show the same binding mode with a small rearrangement in the NS3 structure, as suggested by circular dichroism spectroscopy. These data are consistent with the hypothesis that NS4A complexation induces an NS3 structure that is already (but not entirely) preorganized for substrate binding not only for what concerns the S′ site, as already suggested, but also for the S site. Inhibitor binding to the NS3/cofactor complex induces the stabilization of the enzyme structure as highlighted by limited proteolysis experiments. We envisage that this may occur through stabilization of the individual N-terminal and C-terminal domains where the cofactor and inhibitor, respectively, bind and subsequent tightening of the interdomain interaction in the ternary complex.

Hepatitis C virus (HCV)[1] is the major etiologic agent of transfusion associated and sporadic non-A non-B hepatitis, with the estimation of infected individuals being more than 1% of the world population (*1*). Neither a generally effective therapy nor a vaccine has been developed so far, and much effort is currently devoted to small-molecule drug discovery to eliminate or control HCV infection. In this respect, the inactivation of virally encoded enzymes that are essential for viral replication is generally accepted as the preferential strategy.

The N-terminal third of HCV NS3 protein contains a chymotrypsin-like serine protease (henceforth called NS3 protease) that accomplishes four out of the five processing events necessary for maturation of the nonstructural portion of the viral polyprotein (*2*−*7*).

In vivo, the NS3 protein performs its proteolytic activity by forming a heterodimeric complex with NS4A, a virally encoded 54-residue protein which binds to the N-terminal region of NS3 via a central hydrophobic domain which spans residues 21−34 (*8*−*12*). Complex formation enhances hydrolysis at all sites and is an absolute requirement for efficient processing at the NS4B/NS5A junction (*8*). Several studies have shown that a synthetic peptide encompassing the central region of NS4A is sufficient to elicit full activation of the viral protease (*11, 13*−*16*). Spectroscopic studies (*17*), kinetic analysis (*18*), X-ray crystallography (*19*−*21*), and limited proteolysis experiments (*22*) have highlighted that the NS4A peptide binding causes a structural rearrangement in NS3 protease that results in the correct alignment of the residues which form the catalytic machinery. Substrate specificity studies have shown that the NS3 protease cannot cleave small substrates, the minimal length being a decamer spanning P6−P4′ with a conserved acidic residue in P6, cysteine in P1, serine or alanine in P1′, and a hydrophobic residue in P4′ (*23*−*25*).[2] Kinetic analysis has highlighted that the peptide

† This work was supported in part by Progetto di Ricerca di Interesse Nazionale (PRIN) "Biologia Strutturale" from MURST, Roma, Italy.

* To whom correspondence should be addressed. Telephone: +39 06 91093434. Fax: +39 06 91093225. E-mail: bianchi@irbm.it.

‡ Istituto di Ricerche di Biologia Molecolare P. Angeletti.

§ CNR-Università di Napoli Federico II.

|| Present address: Istituto di Ricerche di Biologia Molecolare P. Angeletti (IRBM), Via Pontina Km 30.600, 00040 Rome, Italy.

[1] Abbreviations: CD, circular dichroism; CHAPS, 3-[(3-cholamidopropyl)dimethylammonio]-1-propanesulfonate; DIEA, diisopropylethylamine; DMAP, *N*′,*N*′-(dimethylamino)pyridine; DTT, dithiothreitol; Fmoc, 9-fluorenylmethyloxycarbonyl; HCMV, human cytomegalovirus; HCV, hepatitis C virus; HOBt, *N*-hydroxybenzotriazole; NS, nonstructural; Pep4A, amino acids 1678−1691 of the HCV polyprotein sequence encompassing the central hydrophobic domain of the NS4A protein sufficient for NS3 activation, with three additional non-HCV N-terminal lysine residues, sequence KKKGSVVIVGRIILSGR-NH_2; PyBOP, (benzotriazol-1-yloxy)tris(pyrrolidino)phosphonium hexafluorophosphate; t-Bu, *tert*-butyl; TFA, trifluoroacetic acid.

[2] We follow the nomenclature of Schechter and Berger (*53*) in designating the cleavage sites as P6−P5−P4−P3−P2−P1...P1′−P2′−P3′−P4′ etc., with the scissile bond between P1 and P1′ and the C-terminus of the substrate on the prime site. The binding sites on the enzyme corresponding to residues P6−P5−P4−P3−P2−P1...P1′−P2′−P3′−P4′ are indicated as S6−S5−S4−S3−S2−S1...S1′−S2′−S3′−S4′ etc.

10.1021/bi991220w CCC: $18.00
Published on Web 09/29/1999

Ac-Asp-Glu-Met-Glu-Glu-Cys-OH, corresponding to the P6−P1 natural cleavage product of the NS4A/NS4B junction, acts as a competitive inhibitor of NS3 with an IC_{50} of 1 μM (*26*). Product inhibition was further exploited by using single-mutant and combinatorial peptide libraries that yielded a series of nanomolar peptide inhibitors (*27*).

There are two general mechanisms through which inhibitors and substrates bind to serine proteases. An "induced-fit" model would apply when a structural reorganization within the enzyme is associated with inhibitor binding, while no conformational change would accompany inhibitor binding in a "lock and key" model. Recent spectroscopic evidence has shown that inhibition of the serine protease of human cytomegalovirus (HCMV) by peptidyl carbonyl compounds is associated with a structural rearrangement of the enzyme (*28*). The crystal structure of the HCMV protease in complex with a peptidomimetic inhibitor (*29*) has revealed large conformational differences from the structure of the free enzyme, which may be important for inhibitor binding. Structural reorganization upon inhibitor binding has been proposed for the inhibition of human leukocyte elastase by peptidyl trifluoromethyl ketones (*30*−*32*) and also for the inhibition of chymotrypsin by the aldehyde chymostatin (*33*). Other studies, however, provide evidence that peptide inhibitors can bind to both chymotrypsin (*34*) and porcine pancreatic elastase (*35, 36*) with a lock and key mechanism. Therefore, the mode of inhibition in the case of serine proteases is still open to debate and deserves further consideration. In this respect, HCV NS3 protease is a notable example, due to the requirement of a protein cofactor. Moreover, NS3 is a multifunctional enzyme which, beyond the serine protease activity contained in the N-terminal third, possesses RNA-stimulated NTPase and helicase activities in the C-terminal region. It has not yet been established whether NS4A is able to modulate the helicase and protease activities, but it is already known that NS4A uncouples the ATPase/ssRNA binding and RNA unwinding activities (*37*).

In this study product-based inhibitors of different potencies spanning P6−P1, P5−P1, and P6−P2 were selected as structural probes to investigate the substrate binding site as well as what influence inhibitor binding exerts on NS3 tertiary structure through circular dichroism spectroscopy and limited proteolysis−mass spectrometry.

MATERIALS AND METHODS

Enzyme Preparation. Escherichia coli BL21(DE3) cells were transformed with a plasmid containing the cDNA coding for the serine protease domain of NS3 (amino acids 1−180 from the HCV J strain, followed by the sequence ASKKKK) under the control of the bacteriophage T7 gene 10 promoter. The protein was purified as previously described (*26*). The purity of the enzyme was assessed to be >95% by silver-stained SDS−PAGE and reverse-phase HPLC on a 4.6 × 250 mm Vydac C4 column. The enzyme preparations were routinely analyzed by mass spectrometry performed on HPLC-purified samples using a Perkin-Elmer API 100 instrument, and N-terminal sequence analysis was carried out using Edman degradation on an Applied Biosystems Model 470A gas-phase sequencer. The NS3J preparation consisted of two components; the minor species corresponded to the intact 1−186 protease (MW = 19 743.1 ± 1.5), whereas the major component showed a molecular mass of 19 540.8 ± 1.1 and was identified as a truncated form of the protease lacking the N-terminal dipeptide Met-Ala.

Peptide Synthesis. Protected amino acids were purchased from Novabiochem (Läufelfingen, Germany), Neosystem (Strasbourg, France), or Synthetech (Albany, NY). Peptide synthesis was performed by Fmoc/t-Bu chemistry on NovaSyn TGR (peptide amides), on NovaSyn TGA (peptide acids), or on a preloaded Fmoc-Cys(Trt)-NovaSyn TGA resin, in the case of Cys C-terminal peptides. The first residue of the C-terminal acid, apart from Cys, was esterified to the TGA resin in the presence of DMAP, according to Atherton and Sheppard (*38*). Peptide assembly was done on a Millipore 9050 Plus synthesizer, using PyBOP/HOBt/DIEA (1/1/2) activation with a 5-fold molar excess of acylants over the resin amino groups and 1 h coupling times. Peptides were cleaved by treatment with 88% TFA, 5% phenol, 2% triisopropylsilane, and 5% water (*39*). Crude peptides were purified by reverse-phase HPLC on a Nucleosyl C18 column (250 × 21 mm, 100 Å, 7 μm) using H_2O/0.1% TFA and acetonitrile/0.1% TFA as eluents. Peptides were characterized by analytical HPLC on an Ultrasphere C18 column (250 × 4.6 mm, 80 Å, 5 μm, Beckman), by mass spectrometry, and by ^{1}H NMR.

As protease cofactor we used the peptide Pep4A, which encompasses the central hydrophobic domain of the HCV NS4A protein and is sufficient for NS3 activation, with three additional N-terminal lysine residues to increase solubility, KKKGSVVIVGRIILSGR-NH_2. The concentration of stock solutions of peptides, prepared in buffered aqueous solution, was determined by quantitative amino acid analysis performed on HCl-hydrolyzed samples.

Limited Proteolysis Experiments. Limited proteolysis experiments were performed at 25 °C, in 50 mM phosphate buffer, pH 7.5, 70 mM NaCl, 2.5 mM DTT, 1% CHAPS, and 15% glycerol, using trypsin, chymotrypsin, endoprotease Lys C, and subtilisin as proteolytic probes. Ternary complexes NS3J/Pep4A/inhibitor were formed by incubating the NS3J/Pep4A complex with a 2:1 or 10:1 molar excess of the individual inhibitor at 25 °C for 15 min prior to proteolytic enzyme addition. Each ternary complex was digested using a 1:100 (w/w) enzyme-to-substrate ratio.

The extent of the enzymatic hydrolysis was monitored on a time-course basis by sampling the incubation mixtures at appropriate time intervals, followed by HPLC fractionation of proteolytic fragments on a Vydac C18 column. Peptides were eluted by means of a linear gradient from 5% to 65% of acetonitrile in 0.1% TFA over 73 min; elution was monitored at 220 and 280 nm. Individual fragment samples were identified by injecting the HPLC fractions into an electrospray ion source (kept at 80 °C) at a flow rate of 10 μL/min, on a Bio-Q triple quadrupole mass spectrometer (Micromass, Manchester, U.K.). Data were analyzed using the MASSLYNX program. Mass calibration was performed by means of the multiply charged ions from a separate injection of horse heart myoglobin (average molecular mass 16 951.5 Da); all masses are reported as average mass.

Circular Dichroism Spectroscopy. Circular dichroism measurements were performed using a Jasco J-710 spectropolarimeter equipped with a cell holder thermostatically controlled by a circulating water bath. Measurements were

Table 1: NS3 Inhibitors Spanning P6−P1, P5−P1, and P6−P2 Analyzed in This Study by Circular Dichroism Spectroscopy (CD) and Limited Proteolysis Mass Spectrometry (MS)

no.	peptide[a]	IC_{50} (μM)[b]	analysis
1	Ac-Asp-Glu-Met-Glu-Glu-Cys-OH	1	CD and MS
2	Ac-Asp-Glu-Dif-Glu-Cha-Cys-OH	0.05	MS
3	Ac-Asp-Glu-Dif-Glu-Cha-OH	117	MS
4	Ac-Asp-Glu-Leu-Glu-Cha-Cys-OH	0.14	CD and MS
5	Ac-Glu-Leu-Glu-Cha-Cys-OH	2.6	CD and MS
6	Ac-Asp-Glu-Met-Glu-Cha-Cys-OH	0.35	CD
7	Ac-Asp-Glu-Leu-Ile-Cha-Cys-OH	0.060	CD
8	Ac-Asp-glu-Leu-Ile-Cha-Cys-OH	0.015	CD

[a] Abbreviations: Cha, β-cyclohexylalanine; Dif, 3,3-diphenylalanine; Glu, D-glutamic acid. [b] IC_{50} values for NS3/Pep4A protease were determined as described in ref *27*. Under our experimental conditions, $K_i \sim 0.5\ IC_{50}$.

recorded at 15 °C, with an 8-s time constant and 5 nm/min and averaged for two acquisitions. The protein concentration was 1.2 mg/mL, and spectra were collected with rectangular quartz cells of 1 cm path length in the near-UV region (320−250 nm) and 0.01 cm path length in the far-UV region (250−190 nm). The concentration of both protein and peptide stock solutions was determined by quantitative amino acid analysis. Results are reported as mean residue ellipticity [Θ] having units of deg cm^2 $dmol^{-1}$ and were calculated using a mean residue weight of 106 Da for NS3. Complex formation of NS3 with either Pep4A or the inhibitors or both was analyzed in 50 mM sodium phosphate buffer, pH 7.5, 15% glycerol, 2% CHAPS, and 3 mM DTT by incubating the protein with increasing amounts of peptides for 10 min at 15 °C. Inhibitors containing aromatic residues in their sequence (peptides 2 and 3 in Table 1) were excluded from this study. Spectra were recorded before and after the addition of Pep4A and/or inhibitors and routinely corrected for the background signal and for dilution effects. It was possible to derive the stoichiometry of 1:1 for each peptide with respect to the protease by following the ellipticity as a function of peptide concentration. In fact, in NS3 and in the NS3/Pep4 complex, the inhibitor and Pep4A saturating conditions equal the protein concentration.

RESULTS

Limited Proteolysis−Mass Spectrometry. The combined use of limited proteolysis and mass spectrometry analysis has recently emerged as a useful probe for the study of the structure and dynamics of proteins, to monitor conformational changes, and to investigate the formation of protein−protein or protein−DNA complexes (*22, 40−44*). We used this approach to probe the interaction of the NS3/Pep4A heterodimer with a series of product-based inhibitors. The overall strategy is based on the evidence that amino acid residues located within exposed and flexible regions of the protein can be recognized by proteases. When comparative experiments were carried out on the NS3/Pep4A complex in the presence and in the absence of peptide inhibitors, differences in the susceptibility of specific cleavage sites were detected, from which protein regions involved in the conformational changes could be inferred.

The product inhibitors used in this study are listed in Table 1. Peptide 1 corresponds to the P_6-P_1 sequence of the C-terminal cleavage product of the NS4A/NS4B junction and represents the most potent natural peptide inhibitor of NS3 protease with a IC_{50} of 1 μM. The remaining peptides were obtained by sequence optimization through the use of combinatorial peptide libraries based on the structure of the natural inhibitor and showed a wide range of inhibitory potencies (*27*).

In all cases, formation of the ternary complex was performed by incubating the NS3/Pep4A pair with either a 2:1 or a 10:1 molar excess of the individual peptide inhibitor at pH 7.5, 25 °C, in the presence of 70 mM NaCl for 15 min prior to protease addition. Trypsin, chymotrypsin, endoprotease Lys C, and subtilisin were selected as proteolytic probes, and the extent of the enzymatic hydrolyses was monitored on a time-course basis by sampling the incubation mixtures at appropriate time intervals followed by HPLC fractionation. Fragments released from the complex were identified by ESMS, leading to the assignment of cleavage sites.

As a first stage, the interaction of the natural inhibitor peptide 1 to the NS3/Pep4A heterodimer was investigated using two different concentrations of the peptide. Figure 1 shows the HPLC profiles of aliquots withdrawn after 60 min of chymotrypsin digestion of the ternary complex when a 2:1 (Figure 1B) or a 10:1 (Figure 1C) molar excess of peptide 1 was added. As a reference, Figure 1A shows the same chymotryptic analysis performed on the NS3J/Pep4A complex in the absence of the inhibitor. To allow for easier comparison, the limited proteolysis data previously obtained on the NS3/Pep4A complex (*45*) are also reported in Table 2. Chromatograms in panels B and C of Figure 1 show the characteristic proteolytic pattern at the N-terminus of NS3 where the presence of fragments 7−186 and 22−186 (peaks 10 and 9 in Figure 1) indicates the occurrence of preferential cleavage sites at Tyr6 and Leu21. With respect to the proteolysis of the NS3/Pep4A heterodimer alone, a slower kinetic of hydrolysis was observed for these residues; moreover, Leu64 and Tyr75, located in the N-terminal domain, were completely protected in the ternary complex as shown by the disappearance of peptide fragment 65−75 (peak 3, panel A). These data suggest that the binding of peptide 1 induced conformational changes that led the complex to adopt a more compact structure. This is also supported by the increase in the E/S ratio (from 1:150 for the NS3/Pep4A to 1:100 for the ternary complex) needed to observe proteolysis.

In the NS3/Pep4A complex at longer hydrolysis time a series of small fragments tend to accumulate. Peaks were identified as peptides 135−154, 155−179, and 160−179 (peaks 6, 5, and 4) from which protease-sensitive sites were recognized at Tyr134, Phe154, and Cys159, respectively (Figure 1A). These sites are located in the C-terminal domain and are involved in substrate binding. Phe154 is located at the bottom of the hydrophobic pocket constituting the NS3J active site and is responsible for the specificity of the protease toward small P1 residues (Cys, Thr). Phe154 and Cys159 are part of the E2 β-strand that interacts with the substrate to form an antiparallel β-sheet. The accessibility of these residues in the NS3J/Pep4A complex suggests that under these conditions the substrate binding site is easily accessible and still endowed with considerable conformational freedom. At lower inhibitor concentration (Figure 1B), chymotryptic cleavages were recognized at Phe154 and Cys159 (peaks 5 and 4), corresponding to fragments 155−179 and 160−179.

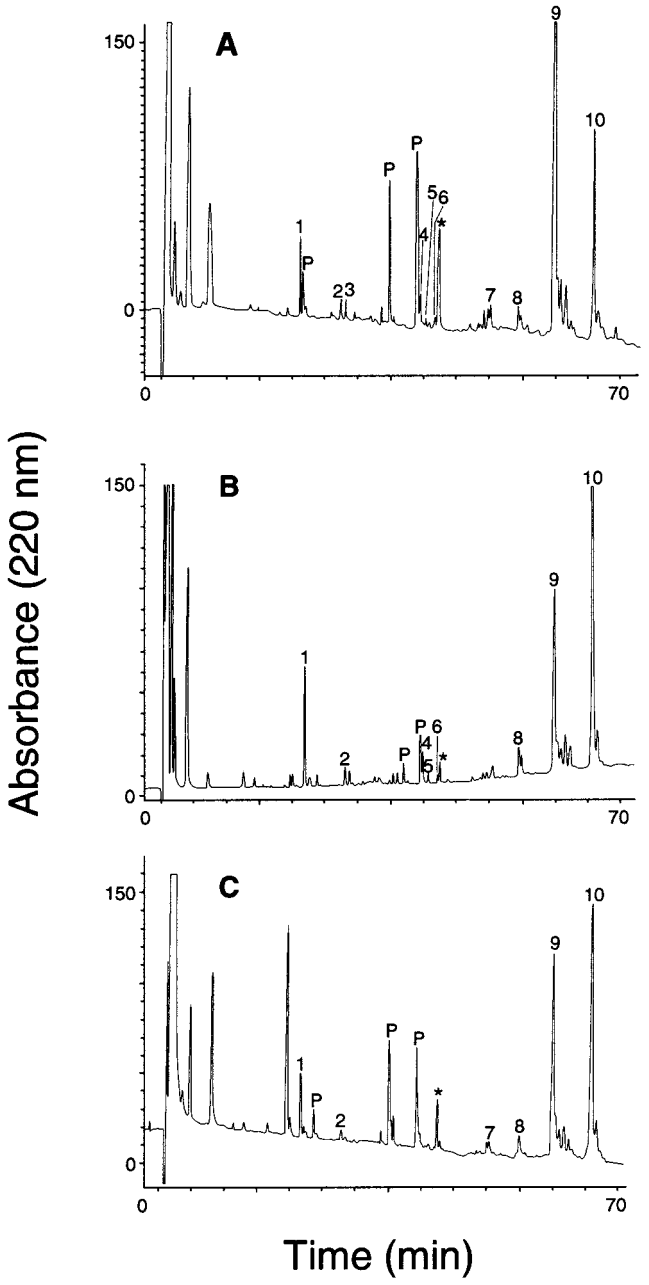

FIGURE 1: HPLC profiles of the NS3/Pep4A complex digested with chymotrypsin in the absence (A) and in the presence of a 2:1 (B) or a 10:1 (C) excess of peptide 1 under controlled conditions using E/S ratios of 1:150 and 1:100, respectively. Individual fractions were collected and identified by ESMS: peak 1 corresponds to NS3 fragment 2−6, peak 2 to 1−6, peak 3 to 65−75, peak 4 to 160−179, peak 5 to 155−179, peak 6 to 135−154, peak 7 to 7−21, peak 8 to 37−186, peak 9 to 22−186, peak 10 to 7−186, and peak 11 to 2−186. The CHAPS peak is marked with an asterisk, peaks marked with P correspond to digestion products of unbound Pep4A, and the inhibitor peak is marked with I.

These peptides were not observed when a higher molar excess of peptide 1 was used (Figure 1C). These data can be correlated with the inhibitory properties of peptide 1; the inhibitor binds to the NS3/Pep4A heterodimer by interacting with the proper binding site, causing the complex to tighten. However, in the presence of a low excess of inhibitor, at equilibrium the ternary complex tends to dissociate, leaving the substrate binding site accessible to chymotrypsin. When a higher concentration of peptide 1 was present, the complex was saturated with the inhibitor and dissociation did not take place, leading to complete protection of the active site against chymotryptic action.

Table 2: Preferential Cleavage Sites Detected on the NS3/Pep4AK Complex in either the Absence or the Presence of a 2:1 Molar Excess of Hexapeptide Inhibitors[a]

cleavage site	NS3/Pep4A	NS3/Pep4A/ Pep1	NS3/Pep4A/ Pep2	NS3/Pep4A/ Pep4
Tyr6	++++	+++	++	+++
Arg11	++++	+++	++	nd[b]
Leu21	+++	++	+	++
Lys26	++++	nd	nd	+++
Arg24	+++	++	++	nd
Lys62	++	−	−	−
Leu64	++	−	−	−
Tyr75	++	−	−	−
Tyr134	++	+	−	−
Phe154	++	+	−	−
Cys159	++	+	−	−
Lys165	+	nd	nd	+

[a] Different cleavage sites were classified merely on qualitative kinetic evaluation. [b] nd = not determined.

Peptide 2 is a more potent peptide inhibitor of NS3 protease, displaying an IC_{50} of 50 nM. Pentapeptide 3 shares the same amino acid sequence with peptide 2 but lacks the C-terminal cysteine residue. The loss of the P1 residue is highly detrimental for binding to the NS3 active site pocket, thus explaining its low inhibitory efficiency ($IC_{50} = 117\ \mu M$) (*27*). However, this peptide still binds in the active site with contacts in the S6−S2 subsites (*46*). Figure 2 shows a comparison of the HPLC profiles of the aliquots withdrawn following 60 min of chymotryptic digestion of the ternary complex formed by the addition of peptide 2 (A) and peptide 3 (B). Again, much slower hydrolysis kinetics as compared to the binary complex was observed in both cases, suggesting that the inhibitors interacted with the proper substrate binding site.

However, a series of differences could be detected in these proteolysis experiments. In particular, when peptide 2 was used, a consistent fraction of intact NS3 could still be observed after 60 min of hydrolysis (peak 11 in Figure 2A). Moreover, only Tyr6 and Leu21, both occurring at the extreme N-terminus of the protease, were recognized by chymotrypsin as preferential cleavage sites; no internal cleavages were, in fact, detected. A quite different situation was observed when the ternary complex was formed with peptide 3. As shown in Figure 2B, besides the N-terminal cleavage sites, chymotrypsin hydrolysis also occurred at Phe154 and Cys159, generating fragments 135−154 and 160−179 (peaks 6 and 4 in Figure 2B) even when a large excess of the peptide inhibitor was present in solution. The hydrolysis and accessibility at Phe154 and Cys159 of peptide 3 suggested that the resulting ternary complex is unstable and tends to dissociate. This result is in agreement with the low IC_{50} value determined for this inhibitor.

Similar results were obtained when the proteolysis experiments were performed using trypsin, endoprotease Lys C, and subtilisin as conformational probes, and the overall data are summarized in Table 2. In particular, tryptic digestion of ternary complexes with either peptide 1 or peptide 2 revealed slower hydrolysis kinetics of Arg11 and Arg24 and complete protection of Lys62 as compared to the proteolysis of the heterodimeric NS3J/Pep4A complex.

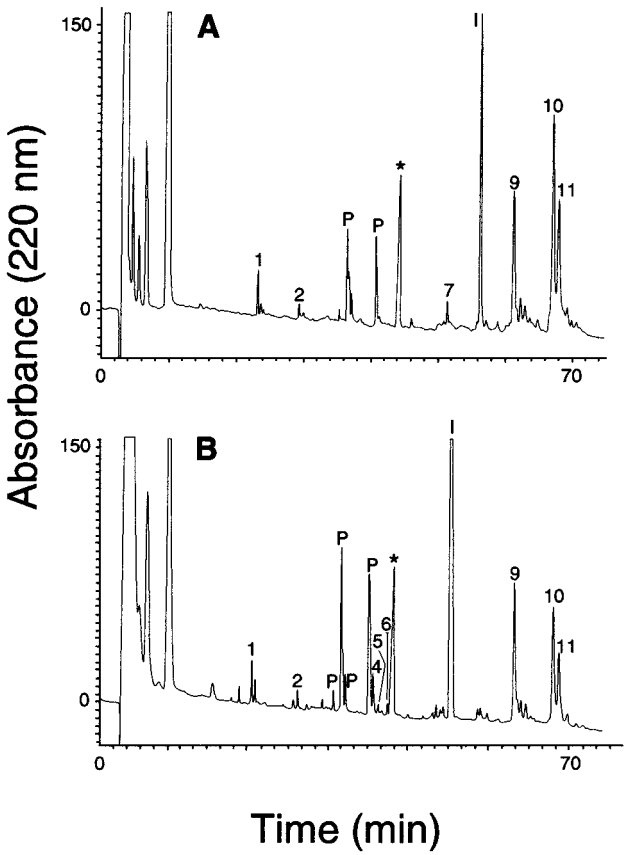

FIGURE 2: Reverse-phase HPLC of the NS3/Pep4A/Pep2 (A) and of the NS3/Pep4A/Pep3 (B) complexes for incubated 60 min with chymotrypsin under controlled conditions using an E/S ratio of 1:100 in the presence of an 1:10 molar excess of each peptide. Individual fractions were collected and analyzed by ESMS; peak numbering is consistent with Figure 1.

One more pair of related peptide inhibitors was investigated. Peptide 4 and peptide 5 share the same amino acid sequence, but the latter lacks the N-terminal Asp residue (P6). This structural difference is reflected in their varying inhibitory capabilities, since the Asp residue is believed to anchor the peptide inhibitor within the substrate binding site by making ionic interactions with the positively charged group of either Arg161 or Lys165. According to these properties, limited proteolysis experiments carried out on the two corresponding ternary complexes showed complete protection of the protease active site by peptide 4 (Table 2). On the contrary, when the complex was formed by peptide 5, both Phe154 and Cys159 were recognized by chymotrypsin (data not shown). Again, these results indicated a dissociation of the ternary complex when the micromolar peptide inhibitor was present in solution. The two complexes were submitted to further limited proteolysis experiments using endoprotease Lys C in order to investigate the peptide anchoring site within the binding region. The results obtained showed a comparable accessibility of Lys165 in both cases, suggesting that the amino acid residue responsible for linking the peptide within the active site might be Arg161. Slower kinetics of hydrolysis at Lys26 and complete protection at Lys62 were also observed in the ternary complex as compared to the NS3/Pep4A heterodimer.

Circular Dichroism Spectroscopy. The contribution of aromatic side chains to the near-UV CD spectra of proteins is widely recognized and utilized as a sensitive probe of protein conformation and ligand binding (*47*, *48*). We used the near-UV CD spectra of the NS3J strain as a probe for monitoring changes in the tertiary structure of the protease upon Pep4A cofactor and inhibitor binding. In the region between 250 and 320 nm the signal in the CD spectrum arises from the aromatic side chains, namely, two tryptophans and five tyrosines of NS3 protease. There is no direct contribution in this spectral region of either Pep4A or the inhibitors used in the CD study (Table 1) since they contain no aromatic residues. Therefore, any change in the near-UV CD region should be interpreted as a perturbation of the environment of the aromatic side chains of NS3 protease.

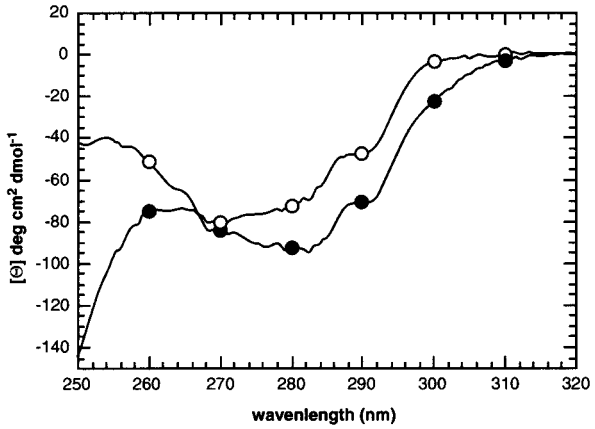

FIGURE 3: Pep4A-induced conformational change of NS3 as detected by near-UV circular dichroism in 15% glycerol, 2% CHAPS, 3 mM DTT, and 50 mM phosphate buffer, pH 7.5: spectrum of NS3 at 60 μM (●) and in the presence of 70 μM Pep4A (○).

NS3J/Pep4A Complex Formation. The formation of the complex between NS3J and Pep4A was studied by monitoring the CD spectra in both the far- and near-UV region. In the case of Bk protease we had already shown (*17*) that Pep4A cofactor complexation is responsible for a large change in the overall near-UV CD spectrum of the protease. The NS3J protease domain differs in eight point mutations from the Bk protease domain. These mutations are single point, are conservative, and do not involve aromatic residues. The comparison of near-UV spectra for Bk and J reveals many differences in the intensity and positions of the bands, while the far-UV spectra are superimposable (data not shown). In this study the formation of the complex between NS3J and Pep4A was followed in 15% glycerol, 2% CHAPS, 3 mM DTT, and 50 mM phosphate buffer, pH 7.5, at a protease concentration of 60 μM. The effect of adding the peptide cofactor to the NS3J protease solution in the near-UV CD region is shown in Figure 3. Also in the case of the J protease, addition of an equimolar amount of Pep4A produces a major change in the 320−250 nm region that reflects a corresponding rearrangement of tertiary structure associated with the mechanism of protease activation by the cofactor. On the other hand, as already reported for NS3 Bk (*17*), no secondary structure changes are evident judging by the far-UV CD in the 250−190 nm region, with identical spectra for NS3J in the presence or absence of the cofactor (data not shown).

Effect of Inhibitors on NS3J. We then analyzed how the binding of inhibitors affected the tertiary structure of the enzyme. All the product inhibitors show competitive binding and bind in the S site of the enzyme. Complex formation

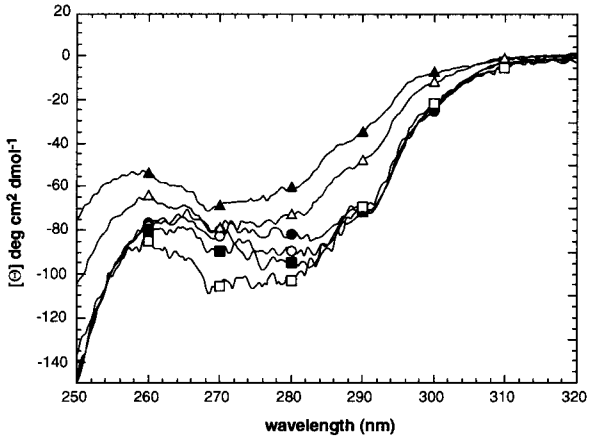

FIGURE 4: Inhibitor-induced conformational change of NS3 as detected by near-UV circular dichroism in 15% glycerol, 2% CHAPS, 3 mM DTT, and 50 mM phosphate buffer, pH 7.5: spectrum of NS3 at 60 μM (●) and with peptide 1 (○), peptide 6 (■), peptide 7 (□), peptide 8 (▲), and peptide 4 (△).

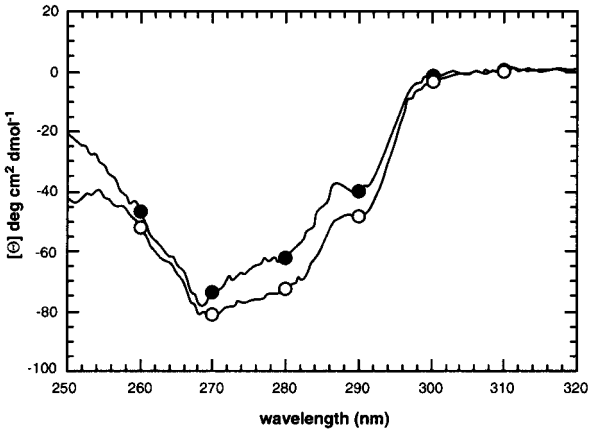

FIGURE 5: Inhibitor-induced conformational change of the NS3/Pep4A complex as detected by near-UV circular dichroism in 15% glycerol, 2% CHAPS, 3 mM DTT, and 50 mM phosphate buffer, pH 7.5: spectrum of the NS3/Pep4A complex (○) and that in the presence of one of the following peptides listed in Table 2: peptide 1, peptide 4, peptide 5, peptide 6, peptide 7, and peptide 8, for which the curves are superimposable (●).

between NS3J and each inhibitor was followed in 15% glycerol, 2% CHAPS, 3 mM DTT, and 50 mM phosphate buffer, pH 7.5, at a protease concentration of 60 μM. In the absence of Pep4A, each inhibitor induces changes in the near-UV CD spectrum of the protease (Figure 4). In particular, peptide 1 and peptide 6 induce a slight increase in intensity between 265 and 285 nm. For peptide 7, the change is more pronounced in intensity in the 260−285 nm region while in the presence of peptides 4 and 8 major differences are present in the overall spectrum. Therefore, a tertiary structure rearrangement of the protease occurs upon binding, suggesting that an induced-fit mechanism is associated with the inhibition process. Moreover, the resulting near-UV CD spectra of various NS3J/inhibitor complexes are different, suggesting that, in the absence of Pep4A, NS3 is quite flexible and adopts different tertiary structures when bound to each individual inhibitor. Thus in the absence of cofactor, these competitive product-based inhibitors bind to NS3 with different binding modes.

Effect of Inhibitors on the NS3J/Pep4A Complex. The effect of the inhibitors on the NS3J/Pep4A complex was analyzed by comparing the near-UV CD spectrum of the binary complex, NS3J/Pep4A, with the spectra of the different ternary complexes NS3J/Pep4A/inhibitor (Figure 5). The near-UV CD spectrum of the NS3J/Pep4A complex is affected by the binding of the product-based inhibitors, showing a slight but reproducible decrease in intensity. More importantly, the spectra of all the ternary complexes are superimposable. The difference between the NS3J/Pep4A complex and the ternary complex indicates a rearrangement of tertiary structure, suggesting that the inhibitors bind to the NS3J/Pep4A complex according to an induced-fit model. However, the structural change may be rather small with respect to the tertiary structure of the NS3J/Pep4A complex. Moreover, all the product inhibitors produce the same qualitative and quantitative change in the spectrum, and hence the inhibitors adopt the same binding mode in the case of the Pep4A-complexed enzyme, despite their inhibitory potency varying in the micromolar to nanomolar range.

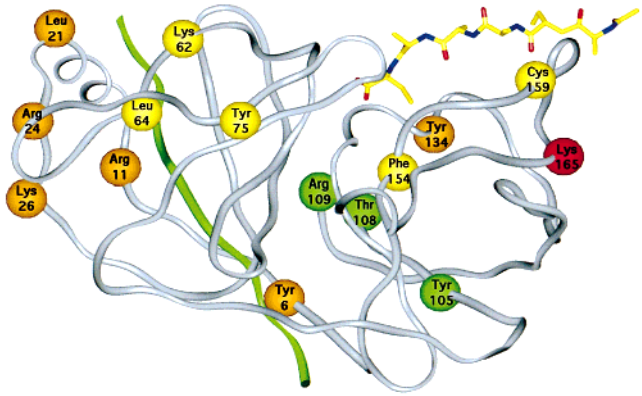

FIGURE 6: Ribbon representation of the backbone of the crystal structure of the NS3 protease/Pep4A complex (*21*). A gray ribbon is used for the backbone of the NS3 protease and a green ribbon for NS4A. The backbone of a hexapeptide product inhibitor modeled on the basis of NMR data (*46*) is shown as a stick presentation. Yellow spheres indicate the positions of amino acids at which the NS3/NS4A complex is proteolytically cleaved and at which cleavage is completely suppressed by peptide 1 and orange spheres those at which cleavage is only partially suppressed by peptide 1. A red sphere is used for the position of Lys165. Cleavage at this position is not influenced by peptide 1. Three positions at which NS3 protease without NS4A is cleaved but no cleavage occurs in the NS3/NS4A complex are shown as green spheres (*45*).

DISCUSSION

Three groups have independently solved the crystal structure of NS3 alone (*19*) and in complex with the Pep4A (*20, 21*). More recently, the NMR solution structure of the isolated NS3 protease domain (*49*) and of NS3/product inhibitor complexes (*46*) has also been reported. However, no structural information is available so far for the ternary complex between the inhibitors and NS3/4A, the most relevant to the observed structure−activity relationships (*27*) and to the design of nonpeptidal drugs. Figure 6 shows the ribbon representation of the crystal structure of the NS3/Pep4A complex (*21*), where the backbone of the hexapeptide product/inhibitor has been modeled on the basis of the NMR data (*46*). In this figure, the cleavage sites from the limited proteolysis data have been highlighted to clarify the following discussion.

On the basis of the structural information available, the rational design of small molecule inhibitors of NS3/4A

appears a challenging task, since the substrate binding region of the enzyme is shallow and entirely solvent exposed, due to lack of the elongated loops connecting the β-sheets that form well-defined pockets in cellular proteases. Accordingly, the NS3 protease cannot cleave small substrates, the minimal length being a decamer spanning P6−P4′ (*23*) with residues distal to the scissile bond contributing significantly to the binding through hydrophobic and electrostatic interactions. These problems notwithstanding, the drug discovery efforts to target NS3/4A have recently yielded potent, cleavage product-based peptide inhibitors (*27*, *50*). The formation of stable enzyme/product complexes has already been described for nonviral serine proteases, in particular for thrombin (*51*, *52*). These structural studies showed that part of the energy which stabilizes inhibitor binding is given by the P1 carboxylate making contacts, via H-bonding, with the catalytic histidine and residues of the oxyanion hole; this is also true for NS3 (*26*, *27*). Moreover, it has been shown (*52*) that, in the case of trypsin, altering the structure of an inhibitor can affect the mode of binding, leading to significant reorganization of protein structure and defining alternative binding motifs.

In the absence of NS4A, the NS3 protease domain folds into two six-stranded β-barrel, trypsin-like domains with the active site in a crevice between the two domains. The S-binding region comprises the region from Arg155 to Lys165, which is located in the C-terminal β-barrel of NS3. NMR and limited proteolysis suggest that, in the absence of Pep4A, the N-terminal β-barrel is particularly flexible, with the 1−23 region completely disordered, while the C-terminal barrel is more structured (*22*, *49*). In the complex with NS3 (*20*, *21*), Pep4A forms a β-strand that intercalates between two β-strands contributed by the N-terminal domain of the enzyme, resulting in a more ordered structure (Figure 6) that in solution is still very flexible in the N-terminal tail (*22*, *45*). This conformational change leads to a rearrangement of the catalytic triad, which has been suggested as being the activation mechanism of NS3 by Pep4A.

Kinetic analysis by Landro and co-workers (*18*) showed that P-region-based inhibitors bind to the enzyme without being affected by the presence of Pep4A, while inhibitors extending to the P′ region are largely influenced by the presence of the cofactor. This would suggest that while the S region, which is part of the enzyme C-terminal domain, is already preorganized without pep4A, formation of the S′ site in the protease N-terminal domain is induced by the cofactor binding.

At variance with these observations, our data support the idea that the S site of the uncomplexed enzyme is still flexible. The near-UV CD data show that, in cofactor-free NS3, binding of the competitive product inhibitors does not only induce a different structure, but one which varies among different inhibitors. These peptides therefore bind to uncomplexed NS3 according to an induced-fit mechanism, suggesting that the S site of the enzyme is still endowed with conformational freedom since it allows a different type of induced fit for each inhibitor.

As already observed for strain Bk, complex formation with Pep4A induces a large conformational rearrangement in the tertiary structure of NS3J, while the secondary structure is not perturbed. As a consequence of this structural change the enzyme becomes more compact and stable. In fact, upon Pep4A complexation, NS3J becomes susceptible to proteolysis at a few specific sites, essentially located at the extreme N-terminal region where Tyr6, Arg11, and Lys26 are the most accessible residues, followed by Leu21 and Arg24. Further protease-sensitive sites are recognized within both the N- and C-terminal domains. In particular, Tyr134, Phe154, and Cys159, located near the substrate binding site within the C-terminal portion of NS3, are still accessible to proteolysis. When these data are compared to those obtained on the isolated NS3J protease (*45*), it is evident that the kinetics of hydrolysis for all these sites is slower than that observed for the cofactor-free protease. Moreover, complete protection was observed for Tyr105, Thr108, and Arg109 (residues in green in Figure 6) located in the interdomain loop and in the C-terminal domain. These data suggest that complex formation with the cofactor also affects the C-terminal domain, stabilizing a structure of the enzyme that is preorganized for substrate binding. However, in the absence of inhibitor, the substrate binding site is still endowed with considerable conformational freedom. Phe154 and Cys159 are part of the E2 β-strand (*46*) with which the substrate and product inhibitors form an antiparallel β-sheet. The flexibility of E2 could therefore be a requisite for the correct positioning of the substrate; in particular, hydrogen bonds in P3 and P5 have been suggested on the basis of the structure−activity relationship studies (*27*).

Near-UV CD analysis shows that binding of product inhibitors to the NS3J/Pep4A complex still occurs according to an induced-fit model, but with a much more modest rearrangement and a final structure of the ternary complex which is the same for all inhibitors, spanning a potency range from micromolar to nanomolar (Table 1). This is in agreement with the limited proteolysis data cited above, suggesting that in the NS3/Pep4A complex the inhibitor binding site is preorganized but underlining that this organization is still not complete and does not fit a rigid lock and key model.

The stability of the ternary complex as assessed by limited proteolysis shows remarkable differences in comparison with uninhibited NS3/Pep4A (Table 2 and Figure 6). The experiments required an increase in proteolytic enzyme-to-complex ratio, despite which intact NS3 protease was present even at longer incubation times. Upon inhibitor binding, protection was observed for residues in the N-terminal domain, such as Lys62, Leu64, and Tyr75, and for residues of the C-terminal domain which are directly implicated in substrate binding, such as Phe154 and Cys159 (residues in yellow in Figure 6). A slower kinetic of hydrolysis was also observed for Tyr6, Arg11, Leu21, Arg24, and Lys26 (residues in orange in Figure 6) which are located in the two N-terminal β-strands as a consequence of the complex tightening as a result of inhibitor binding. The residual flexibility of this N-terminal portion of the protease suggests that the N-terminal and C-terminal domain of the NS4A protein might have a role in the further stabilization of the ternary complex.

Interestingly, Lys165 (residue in red in Figure 6) has a comparable accessibility in the ternary complexes with inhibitors spanning either P6−P1 or P5−P1, suggesting that Lys165 is not making an ionic interaction with the Asp residue (P6) of the inhibitor.

In conclusion, the binding of product-based inhibitors to NS3 occurs according to an induced-fit mechanism. In the absence of cofactor, different binding modes are apparent,

while in the presence of cofactor, all inhibitors bind to NS3, showing the same binding mode with a small rearrangement of NS3 tertiary structure. These observations are consistent with the hypothesis that the binding of the cofactor occurs according to an induced-fit mechanism, inducing an NS3/4A conformation that is already (but not entirely) preorganized for substrate binding. Cofactor complexation does not only affect the S′ site, as previously suggested (*18*), but the S site as well. Conversely, occupancy of the substrate binding site by the product-based inhibitor induces an overall stabilization of the NS3/cofactor complex, influencing also the N-terminal region, which is directly implicated in cofactor binding. This reciprocal influence may be exerted through the stabilization of the N-terminal and C-terminal domains after cofactor and inhibitor binding, respectively, and subsequent tightening of the interdomain interaction.

Kinetic analysis (*26*, *27*), mutagenesis data (*26*), and structural analysis (*46*) have all shown that the mode of binding of the P-region product inhibitors studied in the present work is very similar to the ground-state binding of the corresponding substrates, with additional binding energy provided by the C-terminal carboxylate (*26*, *27*). Therefore, we believe that the conclusions of this study might be extended to the mechanism of substrate binding by the NS3/4A protease.

ACKNOWLEDGMENT

We gratefully acknowledge the contributions of Stefano Acali, Fabio Bonelli, and Silvia Pesci for help with peptide synthesis and characterization. We also thank Riccardo Cortese for useful discussions and critical reading of the manuscript and Manuela Emili for the artwork.

REFERENCES

1. Houghton, M (1996) in *Fields Virology* (Fields, B. N., Knipe, D. M., and Howley, P. M., Eds.) 3rd ed., pp 1035−1058, Raven Press, New York.
2. Tomei, L., Failla, C., Santolini, E., De Francesco, R., and La Monica, N. (1993) *J. Virol. 67*, 4017−4026.
3. Grakoui, A., McCourt, D. W., Wychowski, C., Feinstone, S. M., and Rice, C. M. (1993) *J. Virol. 67*, 2832−2843.
4. Bartenschlager, R. L., Ahlborn-Laake, L., Mous, J. and Jacobsen, H. (1993) *J. Virol. 67*, 3835−3844.
5. Eckard, M. R., Selby, M., Masiarz, F., Lee, C., Berger, K., Crawford, K., Kuo, C., Kuo, G., Houghton, M., and Choo, Q. L. (1993) *Biochem. Biophys. Res. Commun. 192*, 399−406.
6. Hijikata, M., Mizushima, H., Tanji, Y., Komoda, Y., Hirowatari, Y., Akagi, T., Kato, N., Kimura, K., and Shimotohno, K. (1993) *Proc. Natl. Acad. Sci. U.S.A. 90*, 10773−10777.
7. Komoda, Y., Hijikata, M., Tanji, Y., Hirowatari, Y., Mizushima, H., Kimura, K., and Shimotohno, K. (1994) *Gene 145*, 221−226.
8. Failla, C., Tomei, L., and De Francesco, R. (1994) *J. Virol. 68*, 3753−3760.
9. Failla, C., Tomei, L., and De Francesco, R. (1995) *J. Virol. 69*, 1769−1777.
10. Tanji, Y., Hijikata, M., Satoh, S., Kaneko, T., and Shimotohno, K. (1995) *J. Virol. 69*, 1575−1581.
11. Lin, C., Thomson, J. A., and Rice, C. (1995) *J. Virol. 69*, 4373−4380.
12. Bartenschlager, R., Lohmann, V., Wilkinson, T., and Koch, J. A. (1995) *J. Virol. 69*, 7519−7528.
13. Tomei, L., Failla, C., Vitale, R. L., Bianchi, E., and De Francesco, R. (1996) *J. Gen. Virol. 77*, 1065−1070.
14. Shimizu, Y., Yamaji, K., Masuho, Y., Yokota, T., Inoue, H., Sudo, S., and Shimotohno, K. (1996) *J. Virol. 70*, 127−132.
15. Koch, J. O., Lohmann, V., Herian, U., and Bartenschlager, R. (1996) *Virology 221*, 54−66.
16. Butkiewicz, N., Wendel, M., Zhang, R., Jubin, R., Pichardo, J., Smith, E., Hart, A., Ingram, R., Durkin, J., Mui, P., Murray, M., Ramanathan, L., and Dasmahapatra, B. (1996) *Virology 225*, 328−338.
17. Bianchi, E., Urbani, A., Biasiol, G., Brunetti, M., Pessi, A., De Francesco, R., and Steinkühler, C. (1997) *Biochemistry 36*, 7890−7897.
18. Landro, J. A., Raybuck, S. A., Luong, Y.-C., O'Malley, E. T., Harbeson, S. L., Morgenstern, K. A., Rao, G., and Livingston, D. J. (1997) *Biochemistry 36*, 9340−9348.
19. Love, R. A., Parge, H. E., Wickersham, J. A., Hostomsky, Z., Habuka, N., Moomaw, E. W., Adachi, T., and Hostomska, Z., (1996) *Cell 87*, 331−342.
20. Kim, J. L., Morgenstern, K. A., Lin, C., Fox, T., Dwyer, M. D., Landro, J. A., Chambers, S. P., Markland, W., Lepre, C. A., O'Malley, E. T., Harbeson, S. L., Rice, C. M., Murcko, M. A., Caron, P. R., and Thomson, J. A. (1996) *Cell 87*, 343−355.
21. Yan, Y., Li, Y., Munshi, S., Sardana, V., Cole, J., Sardana, M., Steinkühler, C., Tomei, L., De Francesco, R., Kuo, L., and Chen, Z. (1998) *Protein Sci. 7*, 837−847.
22. Orrù, S., Dal Piaz, F., Casbarra, A., Biasiol, G., De Francesco, R., Steinkühler, C., and Pucci, P. (1999) *Protein Sci.* (in press).
23. Steinkühler, C., Urbani, A., Tomei, L., Biasol, G., Sardana, M., Bianchi, E., Pessi, A., and De Francesco, R. (1996) *J. Virol. 70*, 6694−6700.
24. Urbani, A., Bianchi, E., Narjes, F., Tramontano, A., De Francesco, R., Steinkühler, C., and Pessi, A. (1997) *J. Biol. Chem. 272*, 9204−9209.
25. Zhang, R., Durkin, J., Windsor, W. T., McNemar, C., Ramanathan, L., and Le, H. V. (1997) *J. Virol. 71*, 6208−6213.
26. Steinkühler, C., Biasiol, G., Brunetti, M., Urbani, A., Koch, U., Cortese, R., Pessi, A., and De Francesco, R. (1998) *Biochemistry 37*, 8899−8905.
27. Ingallinella, P., Altamura, S., Bianchi, E., Taliani, M., Ingenito, R., Cortese, R., De Francesco, R., Steinkühler, C., and Pessi, A. (1998) *Biochemistry 37*, 8906−8914.
28. Bonneau, P. R., Grand-Maitre, C., Greenwood, D. J., Lagacé, L., LaPlante, S. R., Massariol, M.-J., Ogilvie, W. W., O'Meara, J. A., and Kawai, S. H. (1997) *Biochemistry 36*, 12644−12652.
29. Tong, L., Qian, C., Massariol, M.-J., Deziel, R., Yoakim, C., and Lagace, L. (1998) *Nat. Struct. Biol. 5*, 819−826.
30. Stein, R. L., Strimpler, A. M., Edwards, P. D., Lewis, J. J., Mauger, R. C., Schwartz, J. A., Stein, M. M., Trainer, D. A., Wildonger, R. A., and Zottola, M. A. (1987) *Biochemistry 26*, 2682−2689.
31. Stein, R. L., Strimpler, A. M., Hori, H., and Powers, J. C. (1987) *Biochemistry 26*, 1301−1304.
32. Stein, R. L., Strimpler, A. M., Hori, H., and Powers, J. C. (1987) *Biochemistry 26*, 1305−1314.
33. Stein, R. L., and Strimpler, A. M. (1987) *Biochemistry 26*, 2611−2615.
34. Brady, K., Wei, A., Ringe, D., and Abeles, R. H. (1990) *Biochemistry 29*, 7600−7607.
35. Takahashi, L. H., Radhakrishnan, R., Rosenfield, R. E., Meyer, E. F., Trainer, D. A., and Stein, M. (1988) *J. Mol. Biol. 201*, 423−428.
36. Edwards, P. D., Meyer, E. F., Vijayalakshmi, J., Tuthill, P. A., Andsik, D. A., Gomes, B., and Strimpler, A. (1992) *J. Am. Chem. Soc. 114*, 1854−1863.
37. Gallinari, P., Paolini, C., Brennan, D., Nardi, C., Steinkühler, C., and De Francesco, R. (1999) *Biochemistry 38*, 5620−5632.
38. Atherton, E., and Sheppard, R. C. (1989) *Solid-phase peptide synthesis, a practical approach*, IRL Press, Oxford, U.K.
39. Sole, N. A., and Barany, G. (1992) *J. Org. Chem. 57*, 5399−5403.
40. Zappacosta, F., Pessi, A., Bianchi, E., Venturini, S., Sollazzo, M., Tramontano, A., Marino, G., and Pucci, P. (1996) *Protein Sci. 5*, 802−813.

41. Zappacosta, F., Ingallinella, P., Scaloni, A., Pessi, A., Bianchi, E., Sollazzo, M., Tramontano, A., Marino, G., and Pucci, P. (1997) *Protein Sci*. 6, 1901−1909.
42. Fontana, A., Polverino de Laureto, P., De Filippis, V., Scaramella, E., and Zambonin, M. (1997) *Folding Des. 2*, R17−R26.
43. Scaloni, A., Miraglia, N., Orrù, S., Amodeo, P., Motta, A., Marino, G., and Pucci, P. (1998) *J. Mol. Biol. 277*, 945−958.
44. Scaloni, A., Monti, M., Acquaviva, R., Tell, G., Damante, G., Formisano, S., and Pucci, P. (1999) *Biochemistry 38*, 64−72.
45. Urbani, A., Biasiol, G., Brunetti, M., Volpari, C., Di Marco, S., Sollazzo, M., Orrù, S., Dal Piaz, F., Casbarra, A. R., Pucci, P., Nardi, C., Gallinari, P., De Francesco, R., and Steinkühler, C. (1999) *Biochemistry 38*, 5206−5215.
46. Cicero, D. O., Barbato, G., Koch, U., Ingallinella, P., Bianchi, E., Nardi, M. C., Steinkühler, C., Cortese, R., Matassa, V., De Francesco, R., Pessi, A., and Bazzo, R. (1999) *J. Mol. Biol. 289*, 385−396.
47. Woody, R. W. (1995) *Methods Enzymol. 246*, 34−71.
48. Kahn, P. C. (1979) *Methods Enzymol. 61*, 339−378.
49. Barbato, G., Cicero, D. O., Nardi, M. C., Steinkühler, C., Cortese, R., De Francesco, R., and Bazzo, R. (1999) *J. Mol. Biol. 289*, 370−384.
50. Llinas-Brunet, M., Bailey, M., Fazal, G., Goulet, S., Halmos, T., Laplante, S., Marice, R., Poirier, M., Poupart, M.-A., Thibeault, D., Wernic, D., Lamarre, D. (1998) *Bioorg. Med. Chem. Lett. 8*, 1713−1718.
51. Martin, P. D., Robertson, W., Turk, D., Huber, R., Bode, W., and Edwards, B. F. P. (1992) *J. Biol. Chem. 267*, 7911−7920.
52. Nienaber, V. L., Mersinger, L. J., and Kettner, C. A. (1996) *Biochemistry 35*, 9690−9699.
53. Schechter, I., and Berger, A. (1967) *Biochem. Biophys. Res. Commun. 27*, 157−162.

BI991220W